Energy Materials

Supplementary Materials

Unveiling ion coordination in solid polymer electrolytes through alkyl chain length modulation in lithium salt chemistry

Paul Neumann[1,2,#], Brigette A. Fortuin[1,3,4,#], Elene Sasieta-Barrutia[1,5], Leire Meabe[1,6,*], Lorena Garcia[1], Maria C. Morant-Miñana[1], Maria Forsyth[5,6,7], Margaud Lecuyer[8], Marc Deschamps[8], Yan Zhang[1], Javier Carrasco[1,6,*], Heng Zhang[7,9], Michel Armand[1], María Martinez-Ibañez[1,*]

[1]Centre for Cooperative Research on Alternative Energies (CIC energiGUNE), Basque Research and Technology Alliance (BRTA), Vitoria-Gasteiz 01510, Spain.
[2]Department of Applied Chemistry and Polymer Science & Technology, University of the Basque Country (UPV/EHU), Donostia-San Sebastian 20018, Spain.
[3]Department of Physics, University of the Basque Country (UPV/EHU), Leioa 48940, Spain.
[4]ALISTORE European Research Institute (ALISTORE-ERI), Centre national de la recherche scientifique (CNRS) FR 3104, Amiens 80039, France.
[5]Institute for Frontier Materials, Deakin University, Burwood 3125, Australia.
[6]IKERBASQUE, Basque Foundation for Science, Bilbao 48009, Spain.
[7]POLYMAT, University of the Basque Country UPV/EHU, Donostia-San Sebastián 200018, Spain.
[8]Blue Solutions by Bolloré, Ergué-Gabéric 29500, France.
[9]Key Laboratory of Material Chemistry for Energy Conversion and Storage (Ministry of Education), School of Chemistry and Chemical Engineering, Huazhong University of Science and Technology, Wuhan 430074, Hubei, China.
[#]Authors contributed equally.

[*]**Correspondence to:** Dr. Leire Meabe, Dr. Javier Carrasco, Dr. Maria Martinez-Ibañez, Centre for Cooperative Research on Alternative Energies (CIC energiGUNE), Basque Research and Technology Alliance (BRTA), Vitoria-Gasteiz 01510, Spain. E-mail: lmeabe@cicenergigune.com; jcarrasco@cicenegigune.com; mmartinez@cicenergigune.com

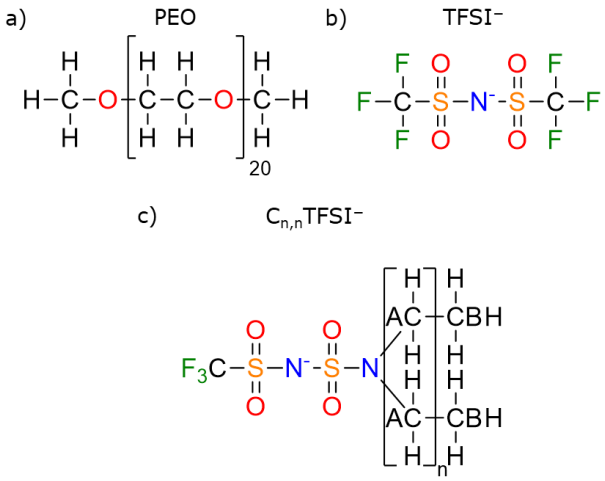

Scheme S1. Chemical structures of (a) PEO, (b) $TFSI^-$ and (c) $C_{n,n}TFSI^-$ with the corresponding adopted acronyms, utilized in MD simulations (Tables S1-S2).

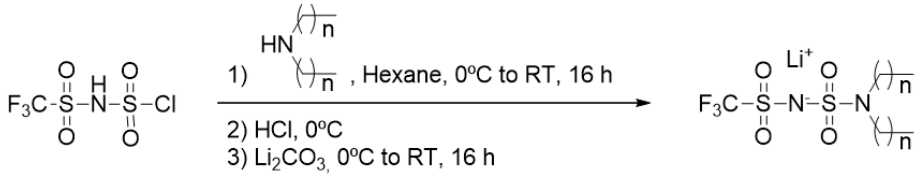

Scheme S2. Synthetic route of the amphiphilic lithium salts.

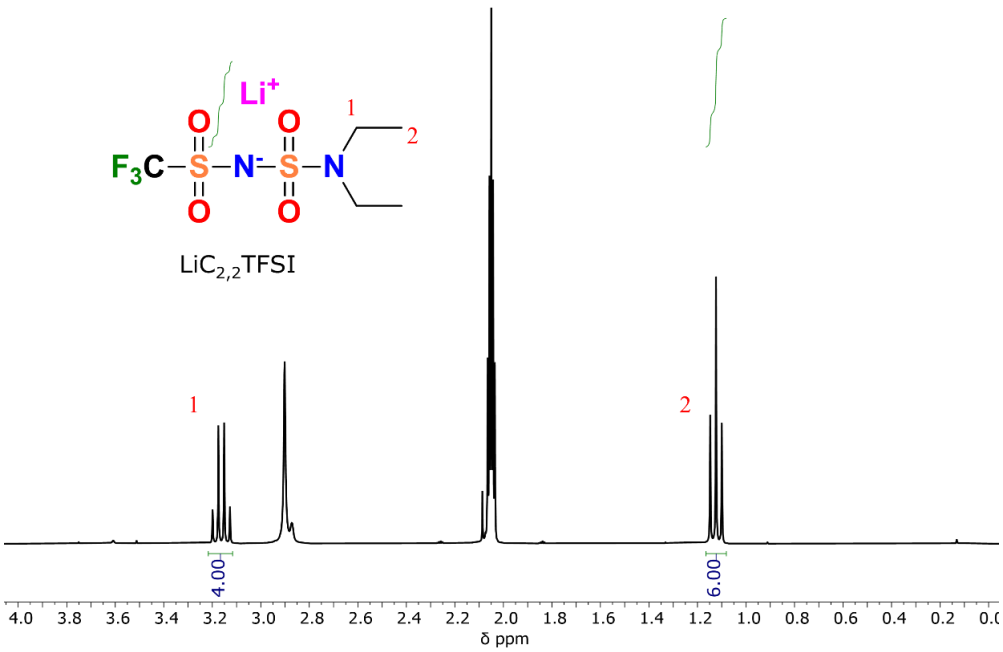

Figure S1. ^1H NMR of $LiC_{2,2}TFSI$.

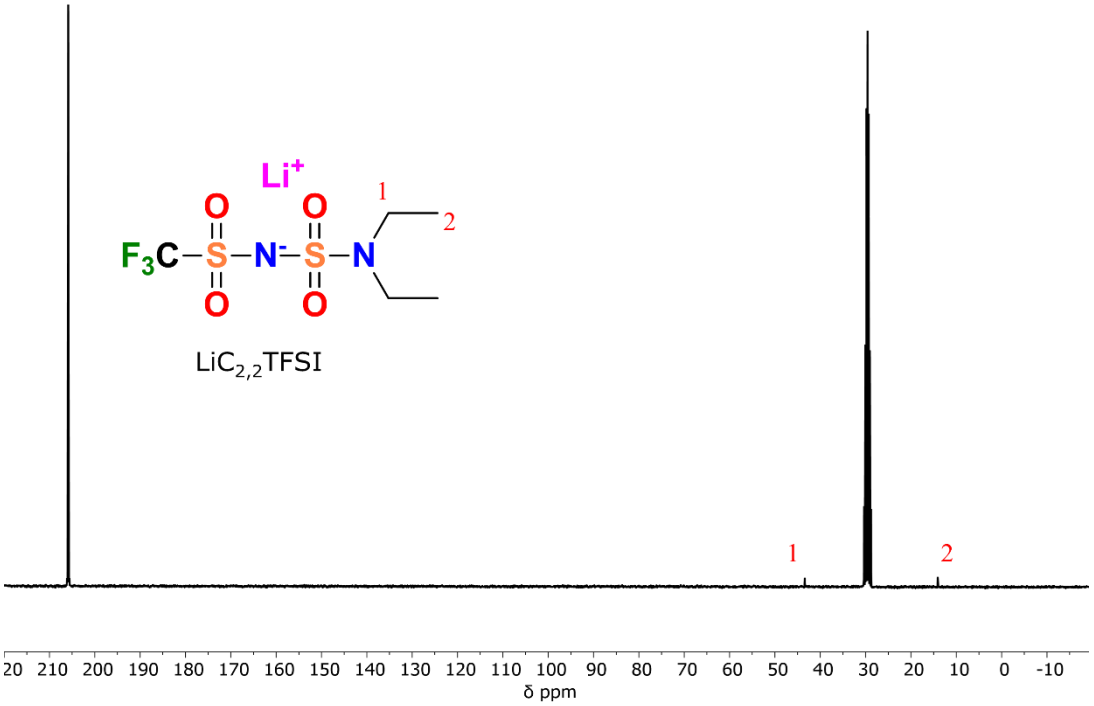

Figure S2. ^{13}C NMR of $LiC_{2,2}TFSI$.

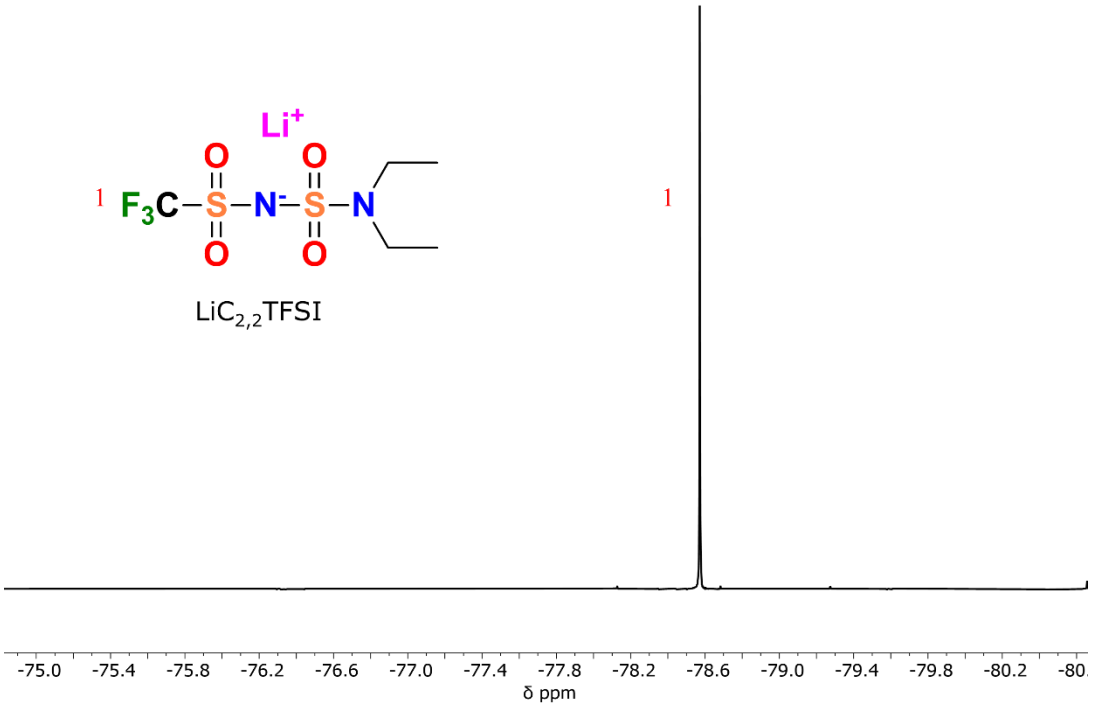

Figure S3. ^{19}F NMR of $LiC_{2,2}TFSI$.

$LiC_{2,2}TFSI$ as a white solid (2.4 g, 8.5 mmol, 67% of yield). ^{1}H NMR (300 MHz, acetone-d_6, ppm): δ = 3.13–3.20 (m,4H, N−C***H*****$_2$**CH_3), 1.10–1.15 (m, 6H, N−CH_2C***H*****$_3$**), ^{13}C NMR (75.5

MHz, acetone-d_6, ppm): δ = 14.10 (N−CH_2***C***H_3), 43.40 (N−***C***H_2CH_3), ^{19}F NMR (283 MHz, acetone-d_6, ppm): δ = −78.57 (s, 3F, C***F*****$_3$**). ICP: lithiation degree = 87 ± 1 %.

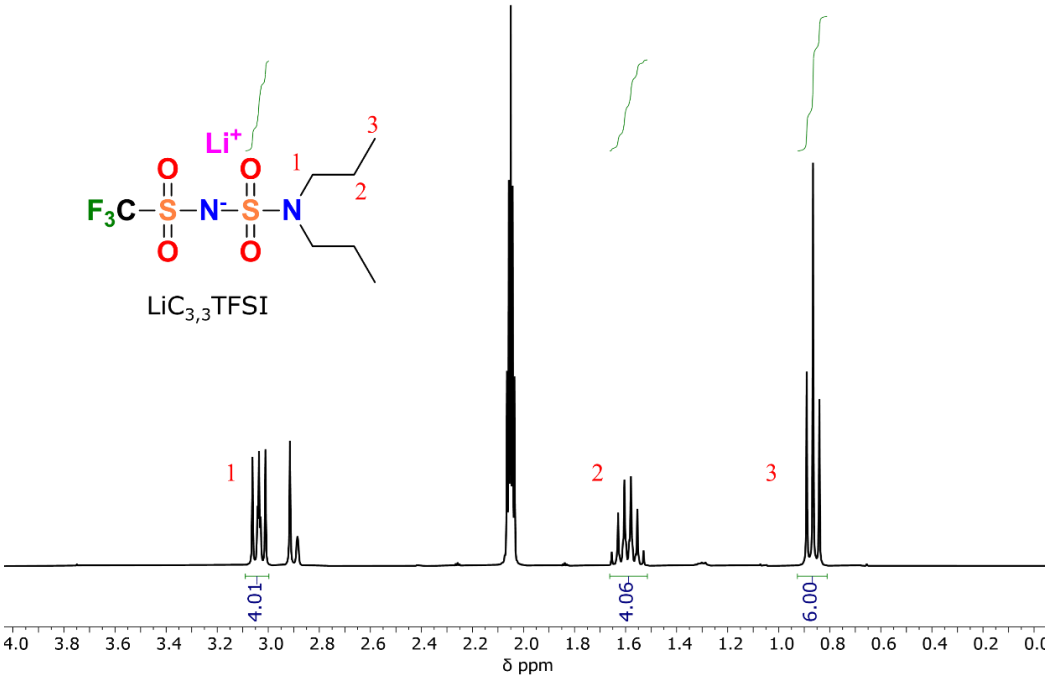

Figure S4. ^{1}H NMR of $LiC_{3,3}TFSI$.

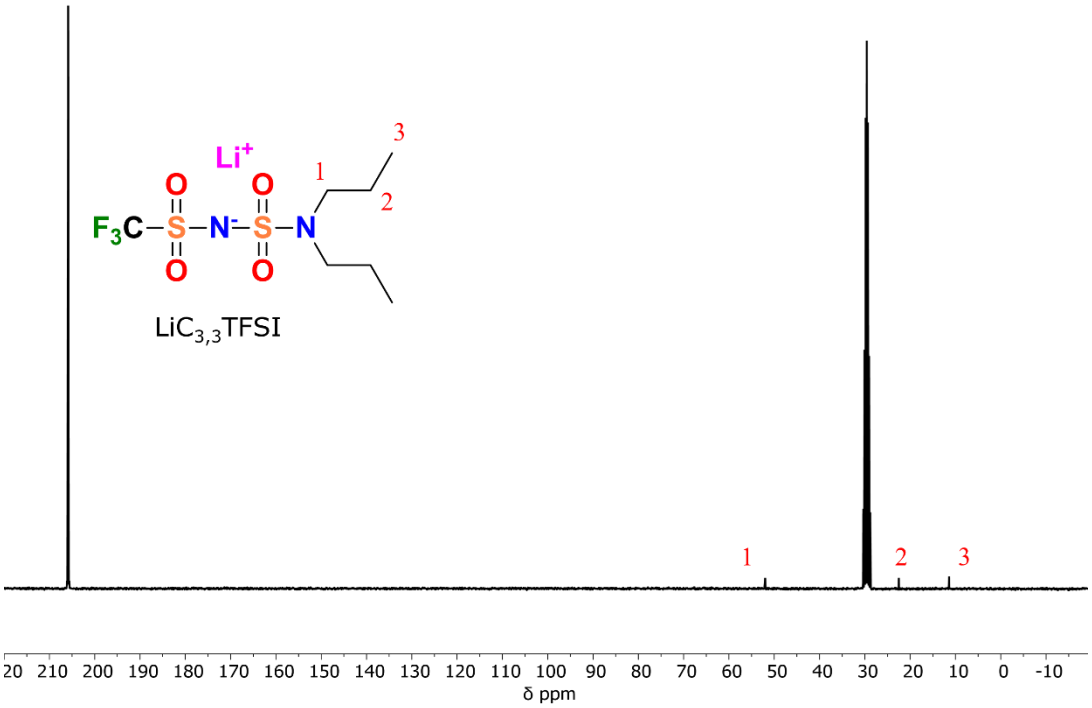

Figure S5. ^{13}C NMR of $LiC_{3,3}TFSI$.

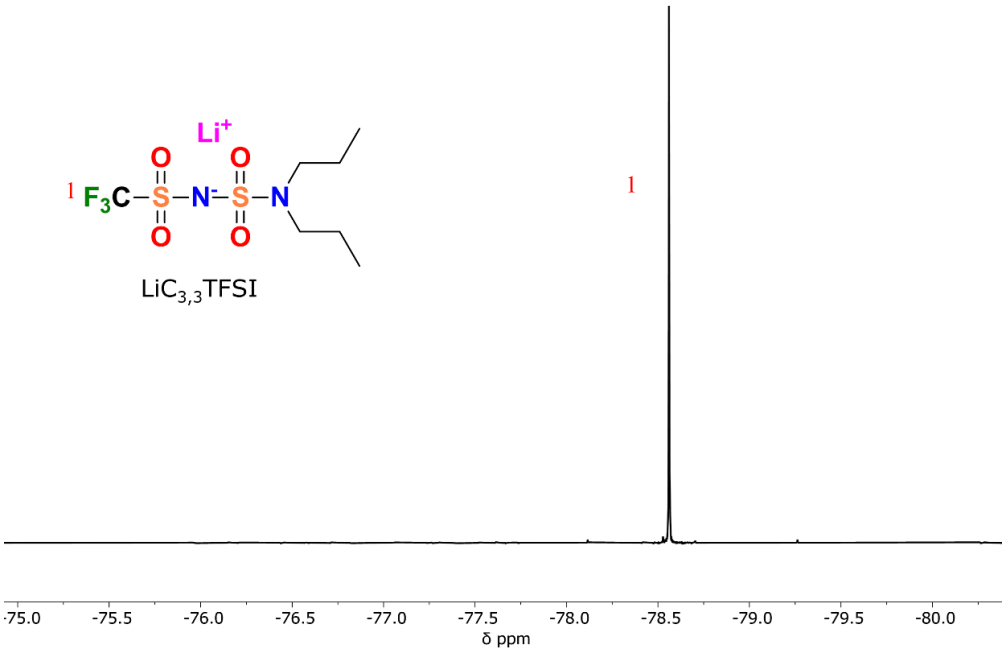

Figure S6. ^{19}F NMR of $LiC_{3,3}TFSI$.

$LiC_{3,3}TFSI$ as a white solid (2.0 g, 6.5 mmol, 67% of yield). ^{1}H NMR (300 MHz, acetone-d_6, ppm): δ = 3.01–3.06 (m, 4H, N−C***H₂***CH_2CH_3), 1.53–1.65 (m, 4H, N−CH_2C***H₂***CH_3), 0.84-0.89 (m, 6H, N−CH_2CH_2C***H₃***), ^{13}C NMR (75.5 MHz, acetone-d_6, ppm): δ = 11.41 (N−CH_2CH_2***C***H_3), 22.50 (N−CH_2***C***H_2CH_3), 51.99 (N−***C***$H_2CH_2CH_3$), ^{19}F NMR (283 MHz, acetone-d_6, ppm): δ = −78.56 (s, 3F, C***F₃***). ICP: lithiation degree = 84 ± 1 %.

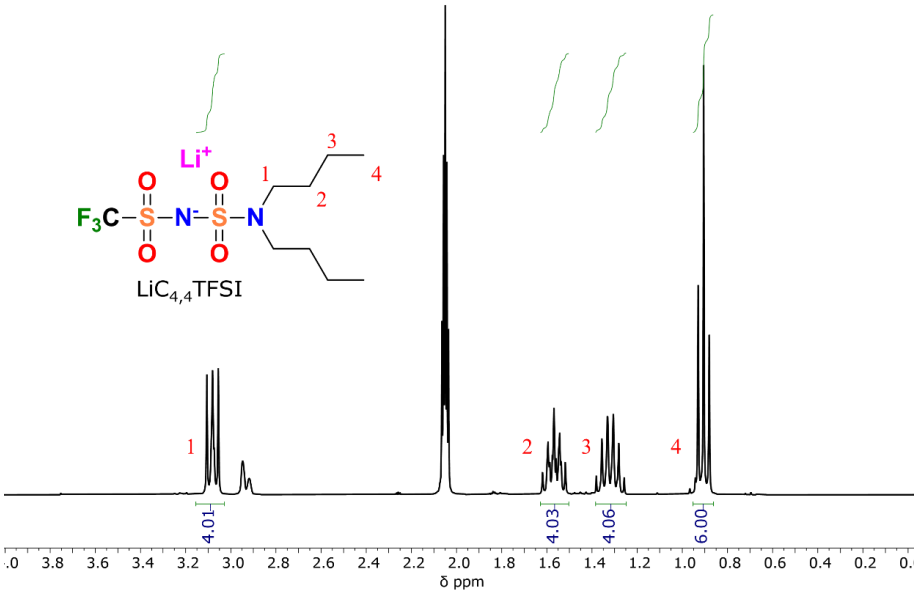

Figure S7. ^{1}H NMR of $LiC_{4,4}TFSI$.

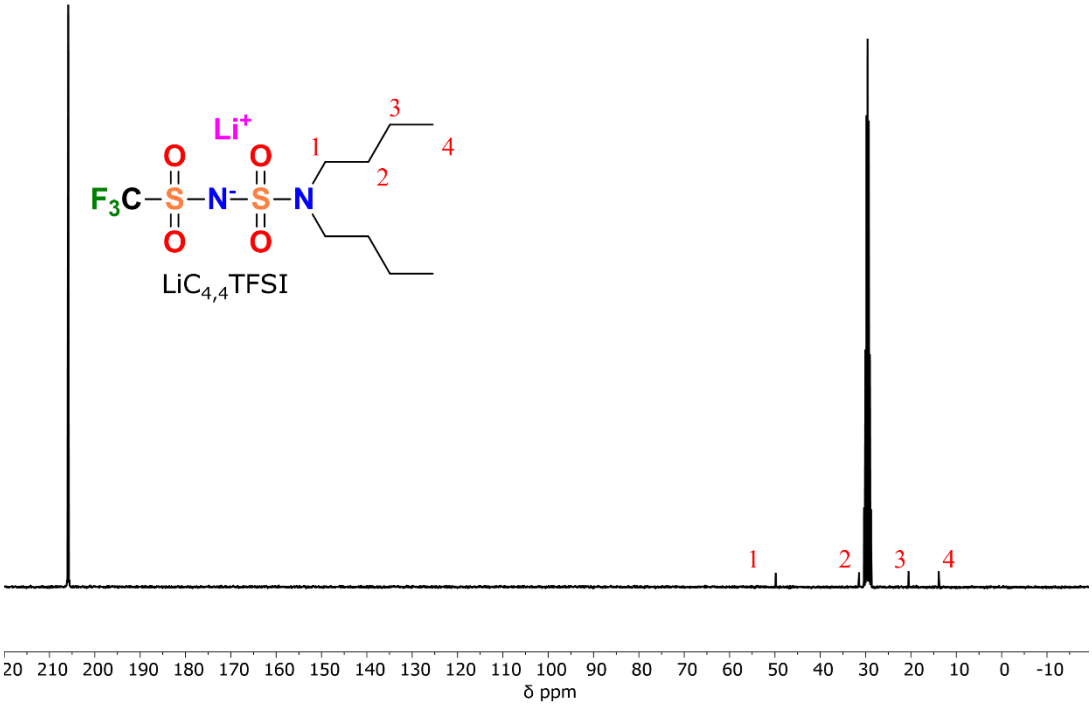

Figure S8. ^{13}C NMR of $LiC_{4,4}TFSI$.

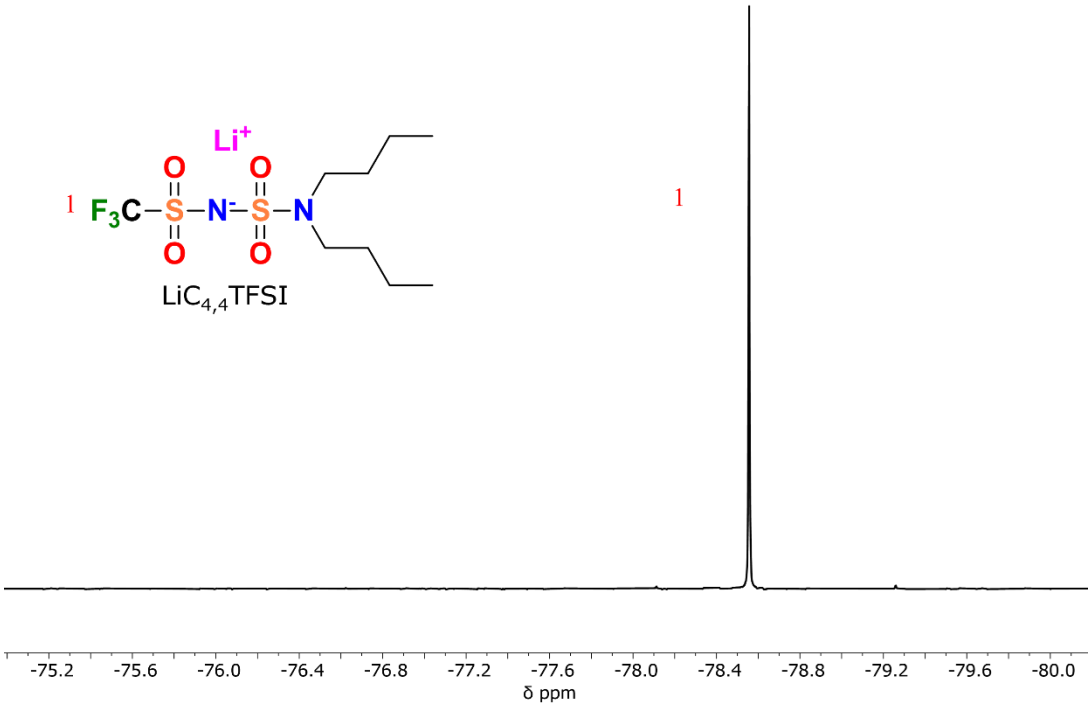

Figure S9. ^{19}F NMR of $LiC_{4,4}TFSI$.

$LiC_{4,4}TFSI$ as a white solid (2.3 g, 6.8 mmol, 47% of yield). ^{1}H NMR (300 MHz, acetone-d_6, ppm): δ = 3.06–3.11 (m, 4H, N−C***H*****$_2$**$CH_2CH_2CH_3$), 1.52–1.62 (m, 4H, N−CH_2C***H*****$_2$**CH_2CH_3),

1.26–1.38 (m, 4H, N−$CH_2CH_2C\boldsymbol{H_2}CH_3$), 0.88–0.93 (m, 6H N−$CH_2CH_2CH_2C\boldsymbol{H_3}$), ^{13}C NMR (75.5 MHz, acetone-d_6, ppm): δ = 13.90 (N−$CH_2CH_2CH_2\boldsymbol{C}H_3$), 20.53 (N−$CH_2CH_2\boldsymbol{C}H_2CH_3$), 31.45 (N−$CH_2\boldsymbol{C}H_2CH_2CH_3$), 49.84 (N−$\boldsymbol{C}H_2CH_2CH_2CH_3$), ^{19}F NMR (283 MHz, acetone-d_6, ppm): δ = −78.56 (s, 3F, C$\boldsymbol{F_3}$). ICP: lithiation degree = 98 ± 1 %.

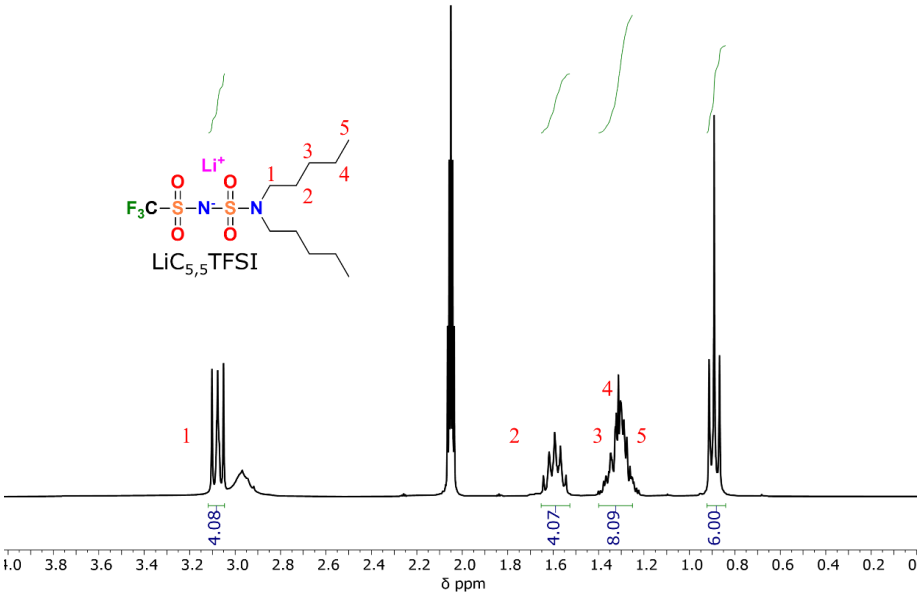

Figure S10. ^{1}H NMR of $LiC_{5,5}TFSI$.

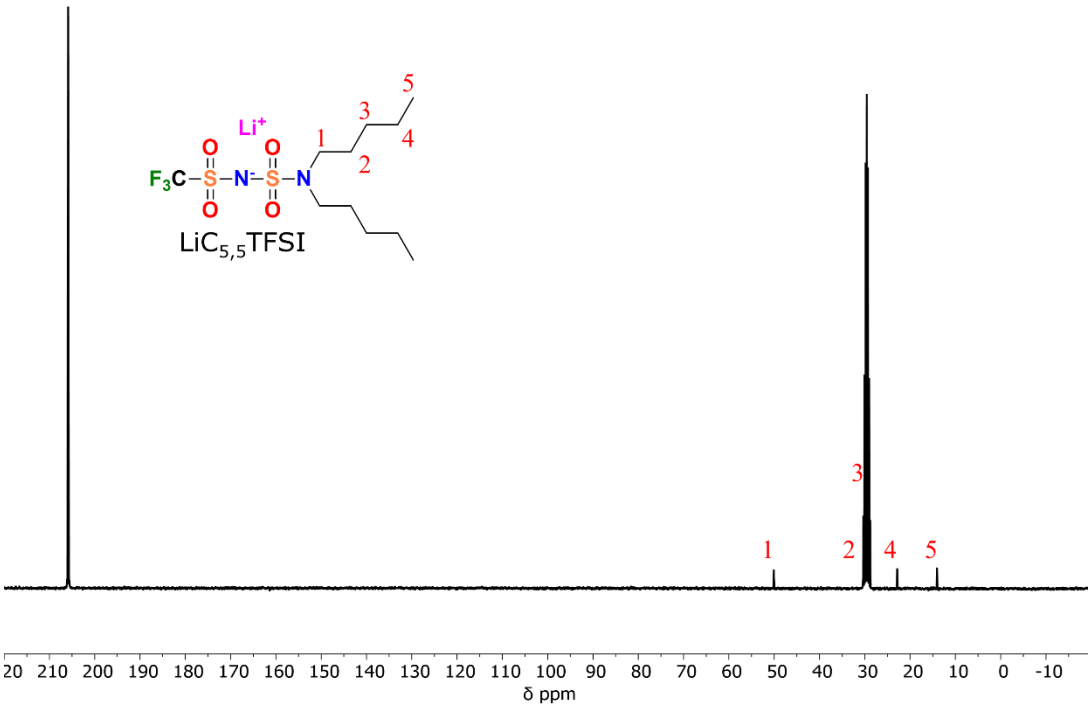

Figure S11. ^{13}C NMR of $LiC_{5,5}TFSI$.

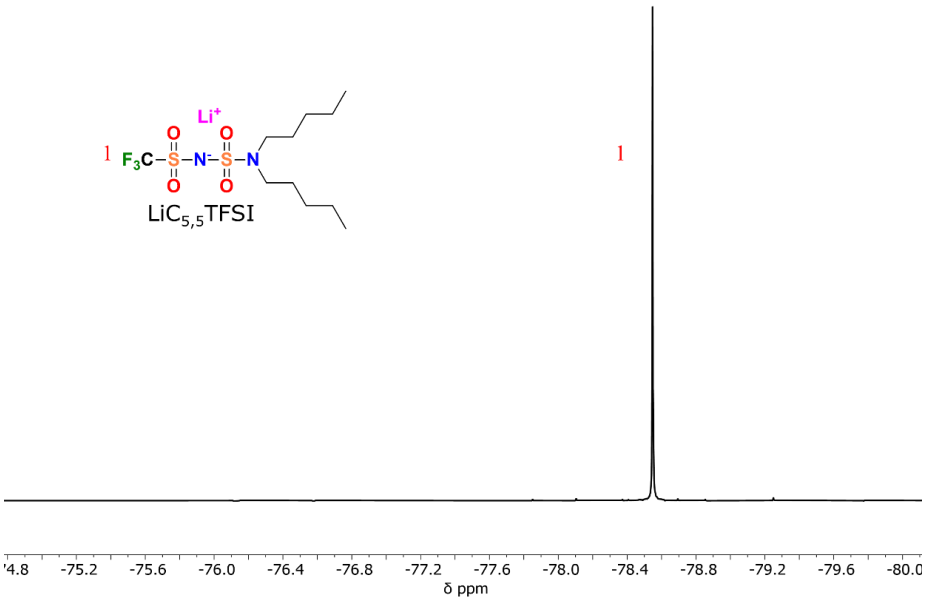

Figure S12. ^{19}F NMR of $LiC_{5,5}TFSI$.

$LiC_{5,5}TFSI$ as a white solid (4.2 g, 11.4 mmol, 83% of yield). ^{1}H NMR (300 MHz, acetone-d_6, ppm): δ = 3.05–3.10 (m, 4H, N−C***H₂***$CH_2CH_2CH_2CH_3$), 1.54–1.62 (m, 4H, N−CH_2C***H₂***$CH_2CH_2CH_2CH_3$), 1.26–1.35 (m, 8H, N−CH_2CH_2C***H₂***C***H₂***CH_3), 0.87–0.91 (m, 6H N−$CH_2CH_2CH_2CH_2$C***H₃***), ^{13}C NMR (75.5 MHz, acetone-d_6, ppm): δ = 14.07 (N−$CH_2CH_2CH_2CH_2$***C***H_3), 22.85 (N−$CH_2CH_2CH_2$***C***H_2CH_3), 28.96 (N−CH_2CH_2***C***$H_2CH_2CH_3$), 29.64 (N−CH_2***C***$H_2CH_2CH_2CH_2CH_3$), 50.07 (N−***C***$H_2CH_2CH_2CH_2CH_3$), (m, J = 324.3 Hz), ^{19}F NMR (283 MHz, acetone-d_6, ppm): δ = −78.55 (s, 3F, C***F₃***). ICP: lithiation degree = 91 ± 1 %.

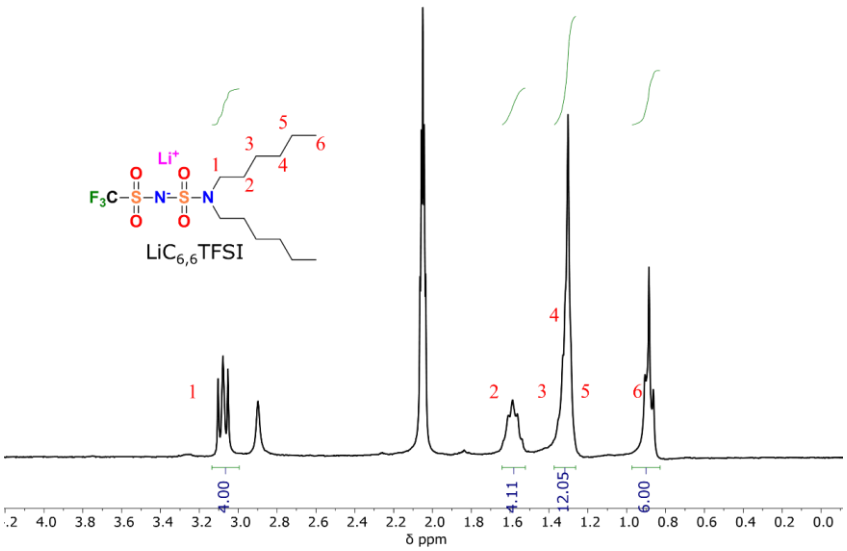

Figure S13. ^{1}H NMR of $LiC_{6,6}TFSI$.

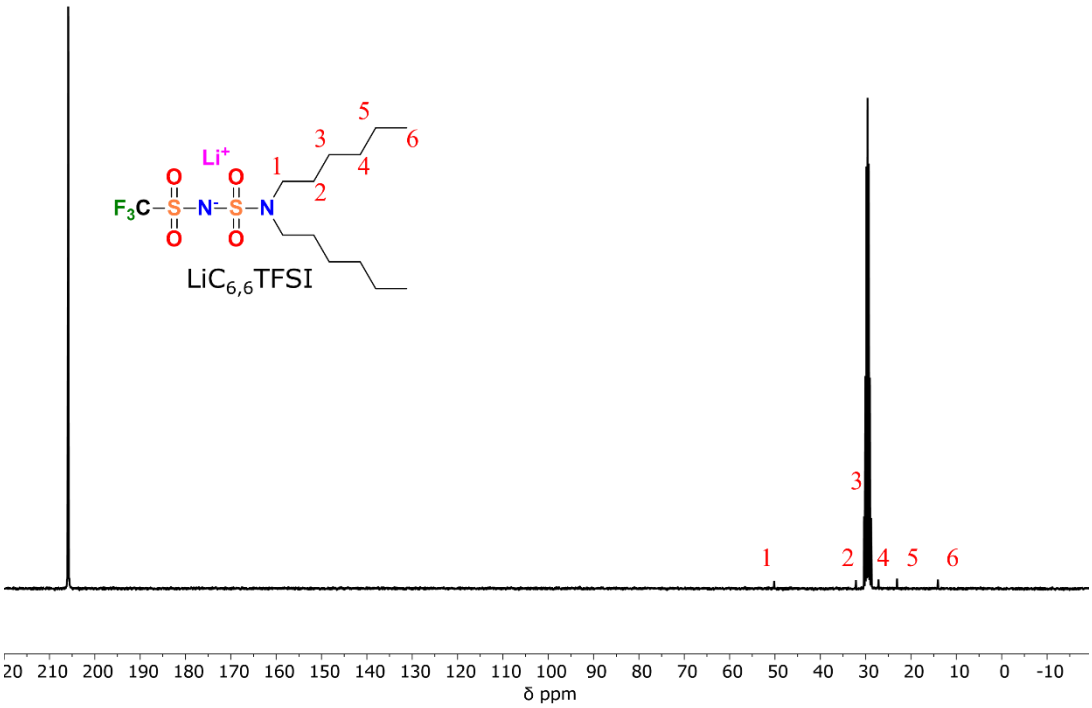

Figure S14. ^{13}C NMR of $LiC_{6,6}TFSI$.

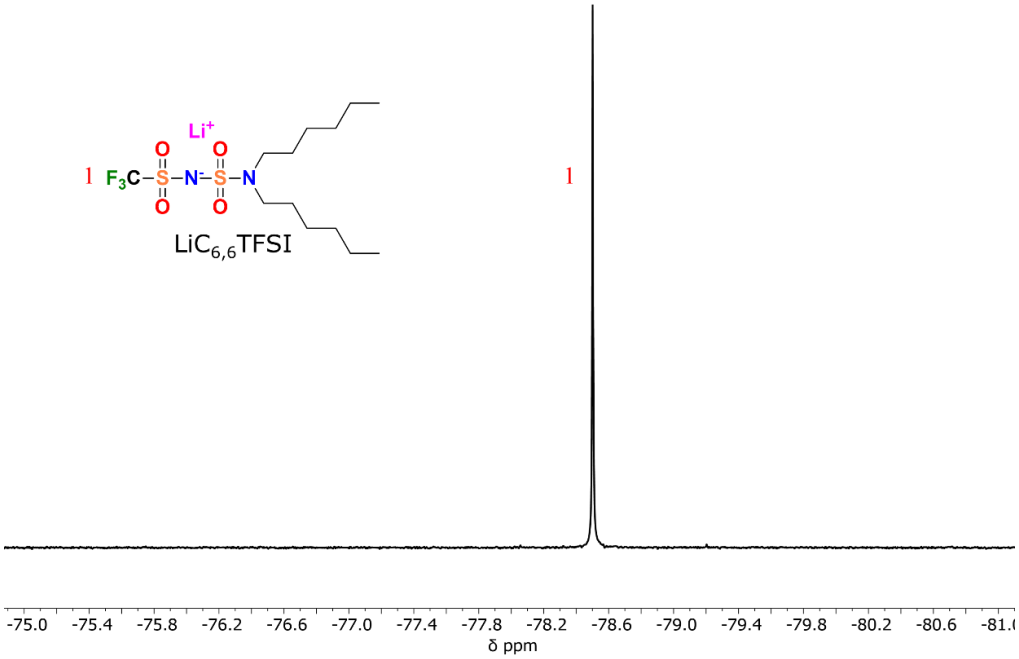

Figure S15. ^{19}F NMR of $LiC_{6,6}TFSI$.

$LiC_{6,6}TFSI$ as a white solid (9.5 g, 24 mmol, 67% of yield). ^{1}H NMR (300 MHz, acetone-d_6, ppm): δ = 3.05–3.10 (m, 4H, N−C***H*₂**$CH_2CH_2CH_2CH_2CH_3$), 1.54–1.63 (m, 4H,

N−$CH_2C\boldsymbol{H_2}CH_2CH_2CH_2CH_3$), 1.28–1.35 (m, 12H, N−$CH_2CH_2C\boldsymbol{H_2CH_2CH_2}CH_3$), 0.86-0.91 (m, 6H N−$CH_2CH_2CH_2CH_2CH_2C\boldsymbol{H_3}$), ^{13}C NMR (75.5 MHz, acetone-d_6, ppm): δ = 13.42 (N−$CH_2CH_2CH_2CH_2CH_2\boldsymbol{C}H_3$), 22.42 (N−$CH_2CH_2CH_2CH_2\boldsymbol{C}H_2CH_3$), 26.51 (N−$CH_2CH_2CH_2\boldsymbol{C}H_2CH_2CH_3$), 28.41 (N−$CH_2CH_2\boldsymbol{C}H_2CH_2CH_2CH_3$), 31.50 (N−$CH_2\boldsymbol{C}H_2CH_2CH_2CH_2CH_3$), 49.54 (N−$\boldsymbol{C}H_2CH_2CH_2CH_2CH_2CH_3$), (m, J = 324.3 Hz), ^{19}F NMR (283 MHz, acetone-d_6, ppm): δ = −78.44 (s, 3F, $C\boldsymbol{F_3}$). ICP: lithiation degree = 87 ± 1 %.

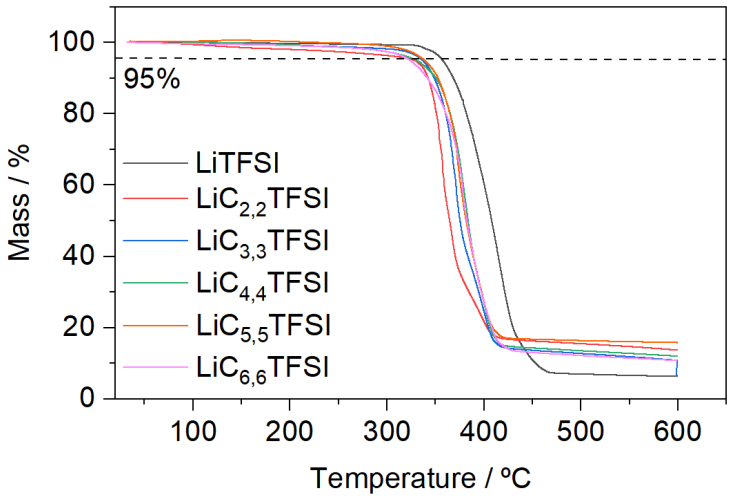

Figure S16. Thermogravimetric analysis (TGA) of the neat salts and LiTFSI at 10 K min^{-1} under argon.

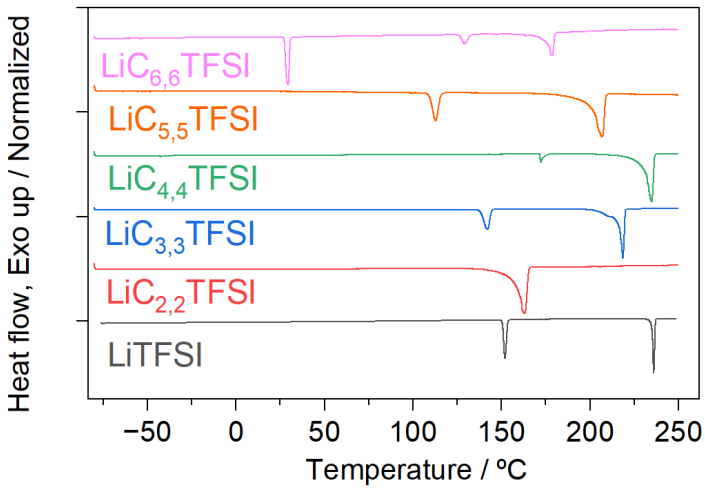

Figure S17. Differential scanning calorimetry (DSC) thermogram (1st heating scan) of the amphiphilic salt family and LiTFSI at a rate of 1 K min^{-1} under argon.

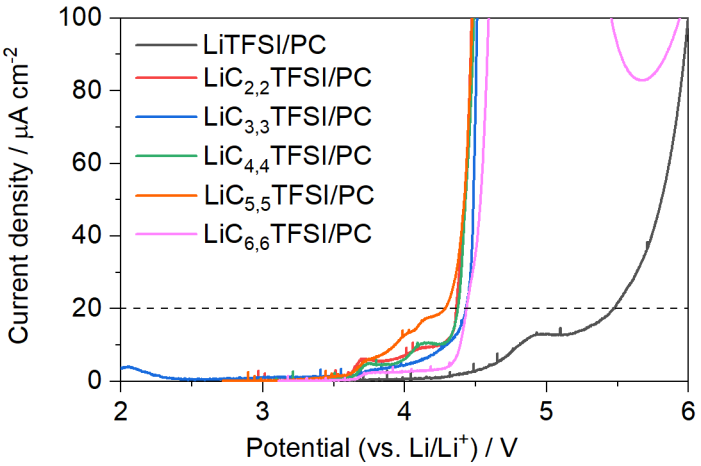

Figure S18. Linear sweep voltammetry (LSV) with 0.1 M of the salts in propylene carbonate (PC) from the open circuit voltage (OCV) to 6.5 V vs. Li/Li^+ at 1 mV s^{-1}.

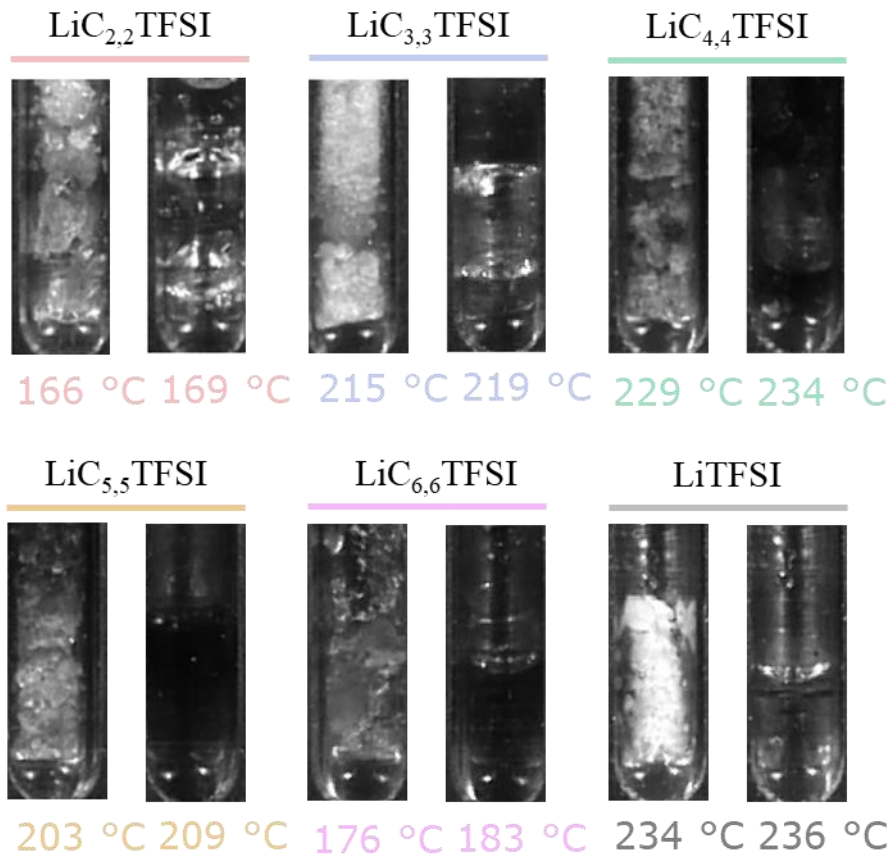

Figure 19. Melting point pictures for each salt obtained with a heating rate of 1 °C min^{-1}.

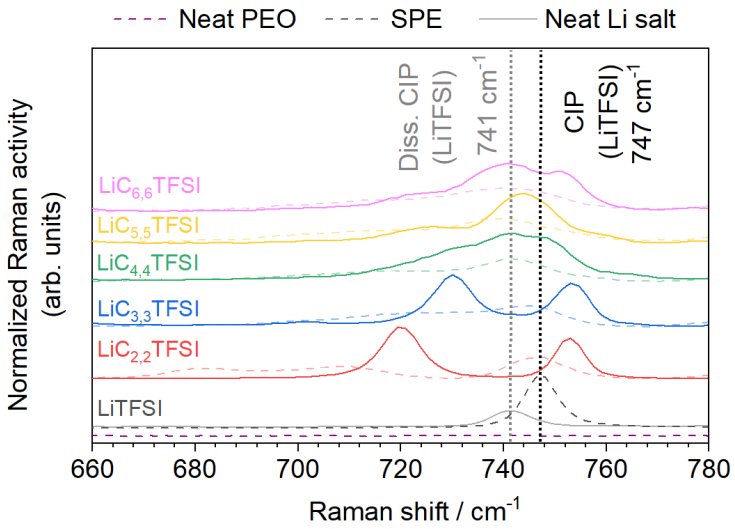

Figure S20. Raman spectra of neat Li salts (25 ºC) and Li salt/PEO SPEs (70 ºC) as a function of $C_{n,n}TFSI^-$ chain length. The vertical dashed lines indicate the contact-ion pair (CIP) (black) and dissociated CIP (grey) for LiTFSI.

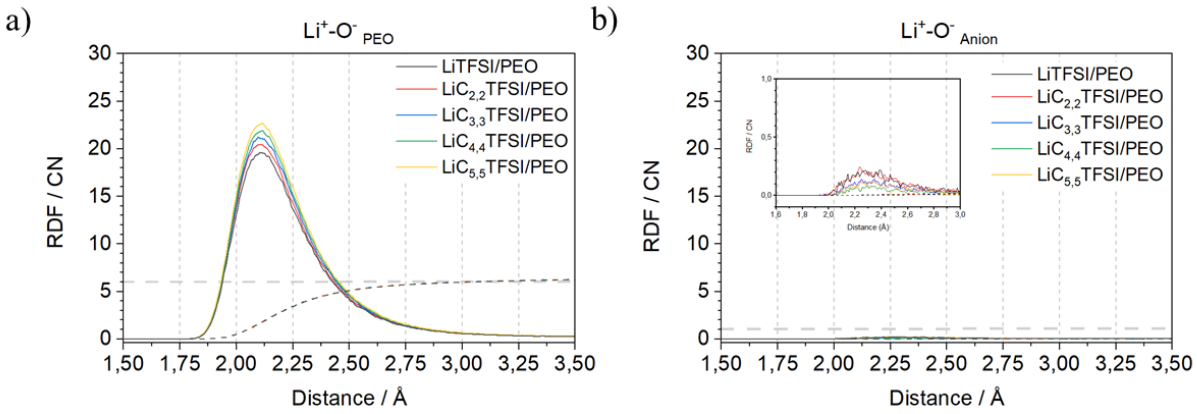

Figure S21. RDFs (solid line) and CNs (dashed line) for LiTFSI/PEO and ($LiC_{n,n}TFSI$)/PEO_n SPEs, indicating the Li^+-O^- interaction between Li ions and (a) PEO and (b) $TFSI^-$, and $C_{n,n}TFSI^-$ ions from MD simulations calculated at 70 ℃.

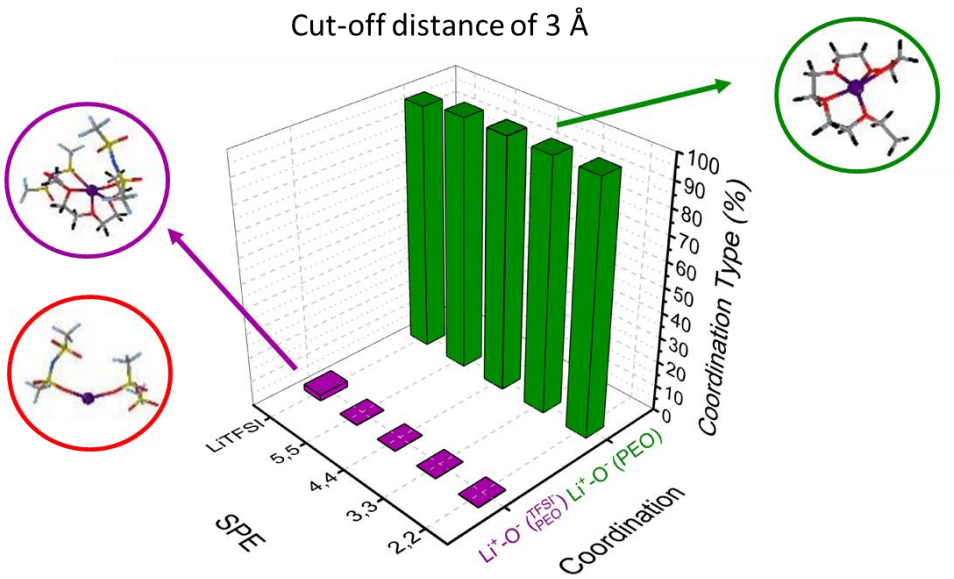

Figure S22. Molecular speciation analysis of the Li-ion with a cut-off distance of 3 Å. The different types of ion speciation are represented by different colours: Li^+-O^-_{PEO} / Anion-O^-_{PEO} (green), Li^+-PEO-Anion (purple), and Li^+-O^-_{Anion} (red).

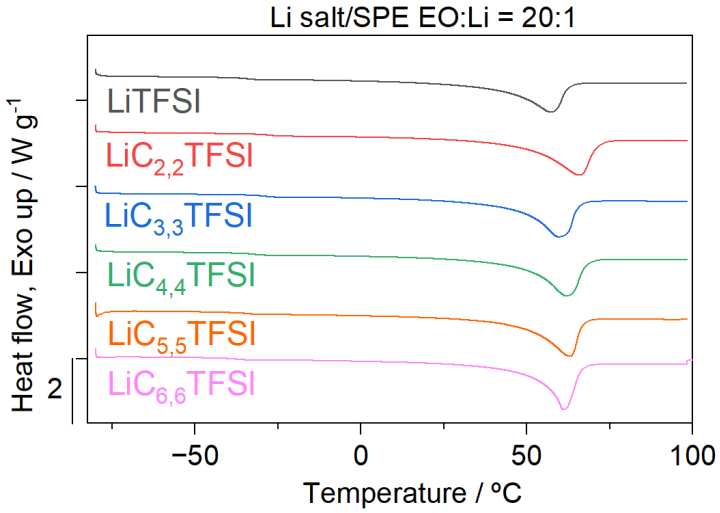

Figure S23. Differential Scanning calorimetry (DSC) thermogram (2nd heating scan) of PEO:Li salts 20:1 (lithium salts: $LiC_{n,n}TFSI$ [2,2 ; 3,3 ; 4,4 ; 5,5 ; 6,6] and LiTFSI) at 10 K min^{-1}.

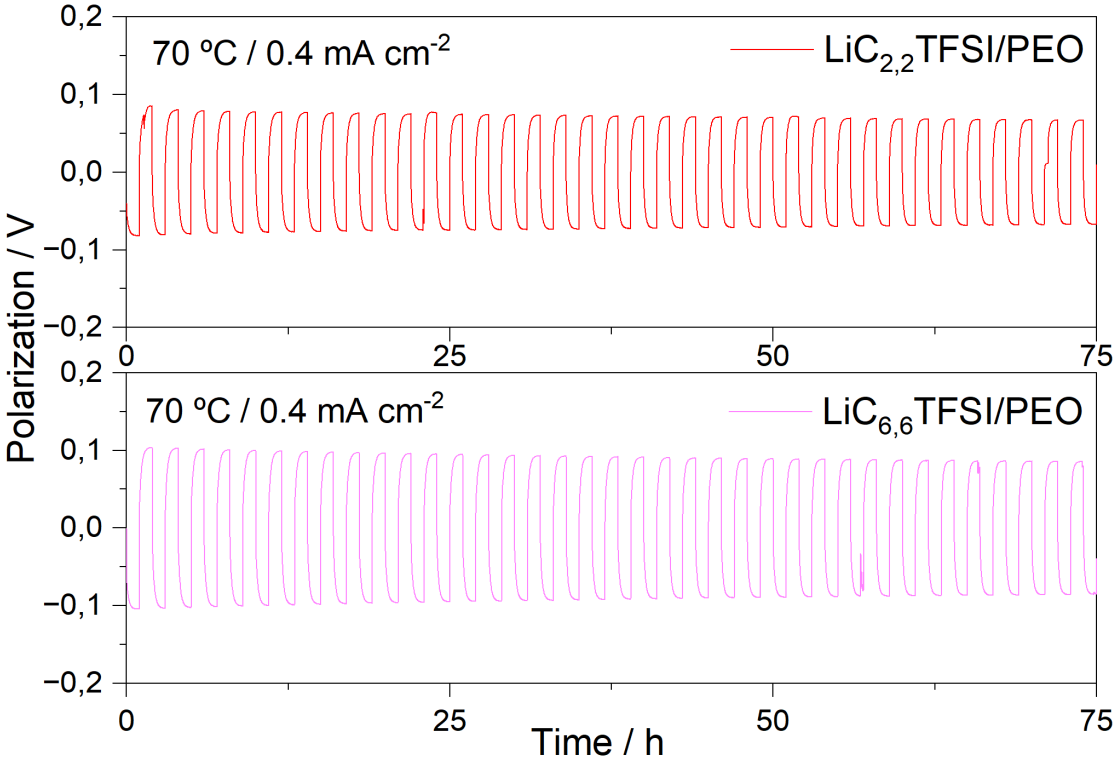

Figure S24. Long term stability of $LiC_{2,2}TFSI/PEO$ and $LiC_{6,6}TFSI/PEO$ at 0.4 mA cm^{-2} at 70 °C.

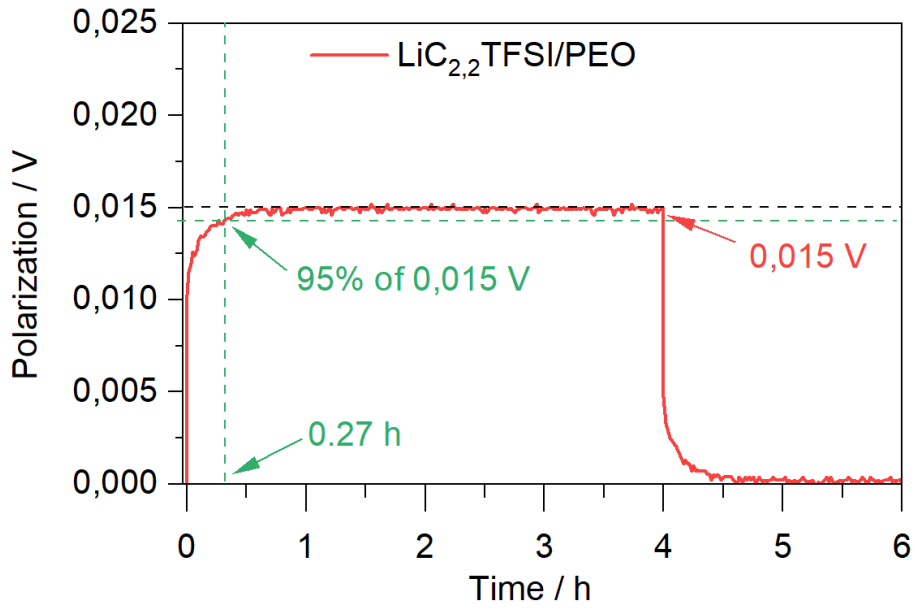

Figure S25. Time to plateau plot of $LiC_{2,2}TFSI/PEO$ under a current density of 0.05 mA cm^{-2}.

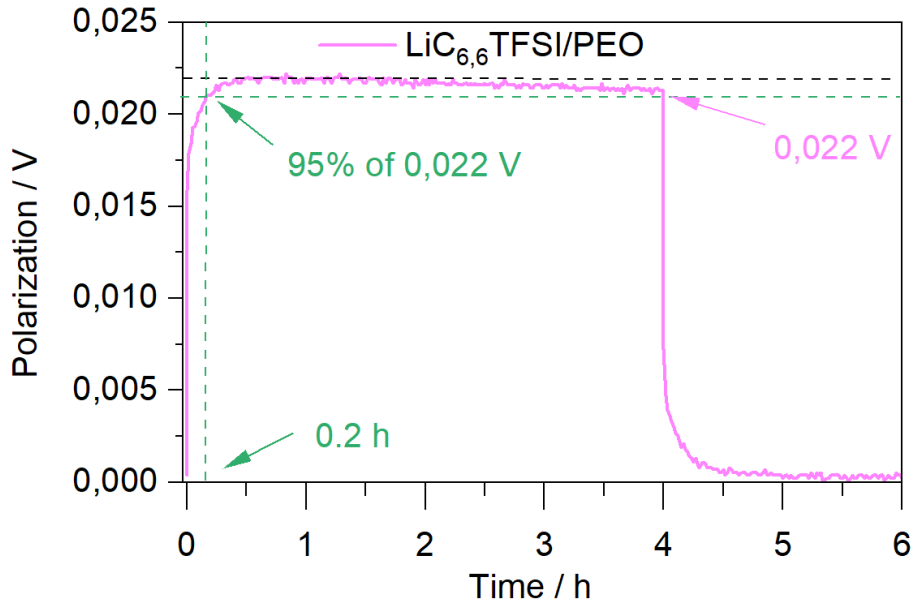

Figure S26. Time to plateau plot of $LiC_{6.6}$TFSI/PEO under a current density of 0.05 mA cm^{-2}.

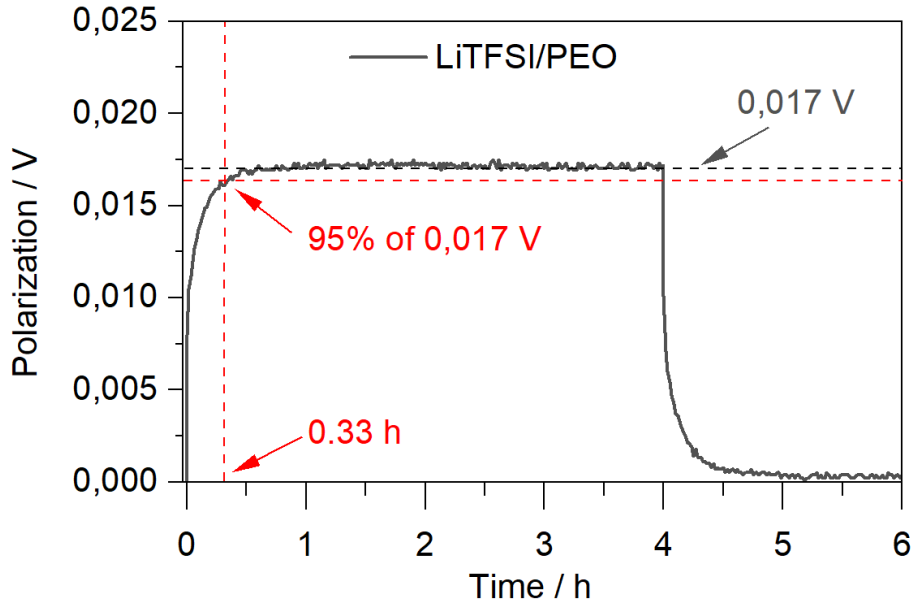

Figure S27. Time to plateau plot of LiTFSI/PEO under a current density of 0.05 mA cm^{-2}.

Table S1. Forcefield parameters for PEO (Fig. S16 (a)) including non-bonded parameters; atomic point charges (*q),* Lennard-Jones parameters, and bonded parameters used in GROMACS simulations.[1,2]

Atom	q e	σ Å	ε $kJ\ mol^{-1}$	**Bond**	r_0 Å	k_r $kJ\ mol^{-1}$ Å^{-2}	**Angle**	θ_0 $degree$	k_θ $kJ\ mol^{-1}$ rad^{-2}
C	−0.18	4.20	0.276	C-C	1.529	2242.624	C-C-H	110.7	313.800
H	0.06	2.50	0.126	C-H	1.090	2845.120	H-C-H	107.8	276.144
O	−0.40	2.90	0.586	C-O	1.410	2677.760	H-C-O	109.5	292.880
C	0.14	3.50	0.276				C-C-O	109.5	418.400
H	0.03	2.50	0.126				C-O-C	109.5	502.080
							C-C-C	112.7	488.273

Dihedral	V_1 $(kJ\ mol^{-1})$	V_2 $(kJ\ mol^{-1})$	V_3 $(kJ\ mol^{-1})$	V_4 $(kJ\ mol^{-1})$
C-C-O-C	1.7154	2.8451	1.0460	−5.6066
H-C-C-H	0.6276	1.8828	0.0	−2.5104
H-C-C-O	0.9791	2.9370	0.0	−3.9162
H-C-O-C	1.5899	4.7698	0.0	−6.3597
O-C-C-O	−1.1506	1.1506	0.0	0.0
C-C-C-H	0.6276	1.8828	0.0	−2.5104
C-C-C-O	2.8744	0.5816	2.0920	−5.5480

Table S2. Forcefield parameters for TFSI($C_{n,n}$TSFI) (Fig. S16 (b) and (c)), including non-bonded parameters, atomic point charges (*q),* Lennard-Jones parameters, and bonded parameters used in both GROMACS.[1–4]

Atom	q e	σ Å	ε $kJ\ mol^{-1}$	**Bond**	r_0 Å	k_r $kJ\ mol^{-1}$ Å^{-2}	**Angle**	θ_0 $degre$	k_θ $kJ\ mol^{-1}$ rad^{-2}
F	−0.16	3.118	0.25540	C-F	1.323	3697.0	F-C-F	107.1	781.0
C	0.35	3.500	0.27614	C-S	1.818	1970.0	F-C-S	111.7	694.0
S	1.02	3.550	1.04600	N-S	1.570	3137.0	C-S-N	103.5	764.0
O	−0.53	3.150	0.83736	O-S	1.437	5331.0	C-S-O	102.6	870.0
N	−0.66	3.250	0.71100	NA-S	1.670	3631.2	N-S-O	113.6	789.0
NA	−0.80	3.250	0.71128	NA-CA	1.449	2820.2	O-S-O	118.5	969.0
CA	0.39	3.500	0.27614	CA-HA	1.090	2845.1	S-N-S	125.6	671.0
HA	−0.06	2.500	0.12552	CB-HB	1.090	2845.1	N-S-NA	104.4	658.3
CB	−0.18	3.500	0.27614	CA-CB	1.529	2246.2	O-S-NA	107.0	1004.2
HB	0.06	2.500	0.12552				S-NA-C	120.0	418.4
Li	0.70	2.126	0.07648				NA-CA(B)-HA	109.5	292.9
							CA-NA-CA	118.0	418.4
							CA(B)-CA-NA	109.7	669.4
							HA(B)-CA(B)-HA(B)	107.8	276.1
							CA-CA(B)-HA(B)	110.7	313.8
							CA-CA-CA(B)	112.7	488.3

Dihedral	$V_1\ (kJ\ mol^{-1})$	$V_2\ (kJ\ mol^{-1})$	$V_3\ (kJ\ mol^{-1})$	$V_4\ (kJ\ mol^{-1})$

F-C-S-N	0.0	0.0	1.322	0.0
F-C-S-O	0.0	0.0	1.451	0.0
S-N-S-C	32.773	−10.420	−3.195	0.0
S-N-S-O	0.0	0.0	−0.015	0.0
S-N-S-NA	0.0	0.0	0.0	0.0
N-S-NA-CA	1.037	−1.483	1.236	0.0
O-S-NA-CA	0.0	0.0	0.0	0.0
S-NA-CA-HA	1.464	−1.266	0.248	0.0
CA-NA-CA-HA	0.0	0.0	0.0	0.0
CB-CA-NA-S	−3.431	−3.008	10.598	−4.159
HA(B)-CA(B)-CA-NA	0.971	2.912	0.0	−3.883
CA(B)-CA-NA-CA	−8.977	−76.686	−8.611	94.274
HA(B)-CA(B)-CA-HA	0.628	1.883	0.0	−2.510
CA(B)-CA-CA-NA	5.487	0.027	0.0	−5.515
CA-CA-CA(B)-HA(B)	0.628	1.883	0.0	−2.510
CA-CA-CA-CA(B)	2.929	−1.464	0.209	−1.674

Table S3. Summary of thermal and electrochemical results of the salts, analyzed by thermogravimetric analysis (TGA) at a heating scan at 10 K min^{-1}, by Differential Scanning calorimetry **(**DSC) thermogram (1st heating scan) at 10 K min^{-1}, by electrochemical impedance spectroscopy (EIS) with 1M of the salts in dimethoxymethane (DME), and by linear sweep voltammetry (LSV) with 0.1 M of the salts in propylene carbonate (PC) from the open circuit voltage (OCV) to 6.5 V vs. Li/Li^+ at 1 mV s^{-1}.

Li Salts	$T_{d,5\%}$ **(°C)**	T_1 **(°C) /** ΔH_1 **(J** g^{-1}**)**	T_2 **(°C) /** ΔH_2 **(J** g^{-1}**)**	T_3 **(°C) /** ΔH_3 **(J** g^{-1}**)**	**Entropy (J** K^{-1} mol^{-1}**) S1 / S2 / S3**	**LSV (V)**
LiTFSI	340	152 / 44	236 / 46	/	30 / 26	5.4
$LiC_{2,2}TFSI$	328	163 / 53	/	/	35	4.4
$LiC_{3,3}TFSI$	337	142 / 24	219 / 62	/	18 / 40	4.4
$LiC_{4,4}TFSI$	330	172 / 3	235 / 57	/	2 / 39	4.4
$LiC_{5,5}TFSI$	338	113 / 17	207 / 48	/	16 / 37	4.4
$LiC_{6,6}TFSI$	323	30 / 35	129 / 11	179 / 39	46 / 11 / 34	4.4

Table S4. Raman deconvolution analysis of neat LiTFSI and $LiC_{n,n}TSFI$ salts based on Raman spectra at 25 ºC.

System	**CIP-C_1 (cm^{-1})**	**CIP-C_2 (cm^{-1})**	**AGG -C_2 (cm^{-1})**
$LiC_{2,2}TFSI$	720.0 ± 0.02	/	752.9 ± 0.02
$LiC_{3,3}TFSI$	729.7 ± 0.1	/	753.2 ± 0.1
$LiC_{4,4}TFSI$	731.3 ± 0.6	741.1 ± 0.3	748.9 ± 0.02
$LiC_{5,5}TFSI$	725.9 ± 0.2	743.8 ± 0.2	755.7 ± 1.4
$LiC_{6,6}TFSI$	722.8 ± 0.4	740.7 ± 0.1	752.5 ± 0.1

Table S5. Raman deconvolution analysis of LiTFSI($C_{n,n}$TSFI)/PEO SPEs based on Raman spectra at 70 ºC.

SPE system	Raman band 1 (%)	Raman band 2 (%)	Raman band 3 (%)
LiTFSI/PEO	100.0 ± 3.0	/	/
$LiC_{2,2}$TFSI/PEO	38.6 ± 6.3	28.1 ± 3.5	33.3 ± 14.3
$LiC_{3,3}$TFSI/PEO	25.5 ± 7.1	74.6 ± 5.1	/
$LiC_{4,4}$TFSI/PEO	34.1 ± 5.1	65.9 ± 13.6	/
$LiC_{5,5}$TFSI/PEO	52.2 ± 4.9	47.8 ± 8.0	/
$LiC_{6,6}$TFSI/PEO	64.3 ± 5.2	35.7 ± 7.6	/

Table S6. Summary of thermal and conductivity results of the electrolytes made of PEO:Li salts 20:1 (lithium salts: $LiC_{n,n}$TFSI [2,2; 3,3; 4,4; 5,5; 6,6] and LiTFSI), analysed by thermogravimetric analysis (TGA) at a heating scan at 10 K min^{-1}, by Differential Scanning calorimetry (DSC) thermogram (2nd heating scan) at 10 K min^{-1}, and by electrochemical impedance spectroscopy (EIS).

Salt:PEO 20:1	$T_{d,5\%}$ (°C)	T_g (°C)	T_m (°C) / ΔH_m (J g^{-1})	X_c (%)	σ_{total} 10^{-4} (S cm^{-1}) at 70 °C	T_{Li^+} EIS at 70 °C	$\sigma_{Li^+}10^{-4}$ (S cm^{-1}) at 70 °C
PEO (Aldrich)	357	−58	67 / 144	73	/	/	/
$LiC_{2,2}$TFSI/PEO	352	−30	66 / 87	59	2.55 ± 0.47	0.43 ± 0.04	1.10 ± 0.30
$LiC_{3,3}$TFSI/PEO	345	−32	60 / 82	57	2.71 ± 0.24	0.44 ± 0.01	1.19 ± 0.13
$LiC_{4,4}$TFSI/PEO	340	−35	62 / 85	60	2.22 ± 0.49	0.48 ± 0.03	1.07 ± 0.31
$LiC_{5,5}$TFSI/PEO	347	−38	63 / 80	58	2.25 ± 0.52	0.48 ± 0.02	1.08 ± 0.30
$LiC_{6,6}$TFSI/PEO	342	−42	63 / 87	65	2.30 ± 0.04	0.52 ± 0.03	1.20 ± 0.09
LiTFSI/PEO	375	−38	57 / 73	49	6.22 ± 0.27	0.21 ± 0.07	1.33 ± 0.50

Table S7. Summary of Li diffusion and T_{Li}^{+} values of PFG NMR and MD simulations at 70 °C.

Li Salt/PEO EO:Li 20:1	**D_{Li+} MD (10^{-8} cm^2 s^{-1})**	**D_{anion} MD (10^{-8} cm^2 s^{-1})**	**t_{Li+} MD**	**D_{Li+} PFG NMR (10^{-8} cm^2 s^{-1})**	**D_{anion} PFG (10^{-8} cm^2 s^{-1})**	**t_{Li+} PFG NMR**
$LiC_{2,2}$TFSI/PEO	2.00 ± 0.75	8.17 ± 1.14	0.22 ± 0.02	4.15	8.00	0.34
$LiC_{3,3}$TFSI/PEO	3.42 ± 1.15	8.38 ± 1.92	0.29 ± 0.02	4.47	6.67	0.40
$LiC_{4,4}$TFSI/PEO	2.25 ± 0.75	4.05 ± 0.84	0.37 ± 0.05	4.30	6.62	0.39
$LiC_{5,5}$TFSI/PEO	2.30 ± 0.13	3.59 ± 0.49	0.39 ± 0.04	4.27	6.21	0.41
$LiC_{6,6}$TFSI/PEO	/	/	/	4.11	5.70	0.42
LiTFSI/PEO	2.65 ± 0.49	11.60 ± 1.59	0.20 ± 0.03	2.40	12.69	0.16

Table S8. T_{Li}^{+} and ionic conductivities obtained by EIS and CA at 40 and 70 °C.

Li Salts	**EO:Li**	**T_{Li}^{+} at 40 °C**	**σ_{total} 10^{-6} / S cm^{-1} at 40 °C**	**σ_{Li}^{+} 10^{-6} / S cm^{-1} at 40 °C**	**T_{Li}^{+} at 70 °C**	**σ_{total} 10^{-4} / S cm^{-1} at 70 °C**	**σ_{Li}^{+} 10^{-4} / S cm^{-1} at 70 °C**
LiTFSI	20:1	0.19 ± 0.02	46.5 ± 1.8	7.52 ± 3.27	0.21 ± 0.07	6.22 ± 0.27	1.33 ± 0.50
$LiC_{2,2}$TFSI	20:1	0.42 ± 0.02	9.60 ± 1.90	4.03 ± 1.90	0.43 ± 0.04	2.55 ± 0.47	1.10 ± 0.30
$LiC_{6,6}$TFSI	20:1	0.51 ± 0.05	7.16 ± 0.93	2.83 ± 0.93	0.52 ± 0.02	2.30 ± 0.41	1.20 ± 0.09

Table S9. Total diffusion given by electrochemical impedance spectroscopy (EIS) and calculated with the Nernst-Einstein relation at 70 °C.

Li Salt/PEO EO:Li 20:1	**D_{total} EIS (10^{-8} cm^2 s^{-1}) at 70 °C**	**D_{Li^+} EIS (10^{-8} cm^2 s^{-1}) at 70 °C**	**D_{anion^-} EIS (10^{-8} cm^2 s^{-1}) at 70 °C**
LiTFSI/PEO	15.78	3.37	12.41
$LiC_{2,2}$TFSI/PEO	6.86	2.99	3.97
$LiC_{6,6}$TFSI/PEO	7.23	3.77	3.46

Table S10. Comparison between lithium diffusion and lithium-ion conductivity calculated by two methods: sand method vs. EIS, at 40 °C. 1st column: lithium diffusion calculated from Sand method and; 2nd column: lithium-ion conductivity calculated from lithium diffusion using the Nernst-Einstein equation; 3rd column lithium diffusion calculated with the Nernst-Einstein from the lithium-ion conductivity estimated from electrochemical impedance spectroscopy (EIS); 4th column: lithium-ion conductivity estimated from electrochemical impedance spectroscopy (EIS)

	Results derived from Sand method		**Results derived from EIS measurements**	
Li Salt/PEO EO:Li 20:1	**D_{Li+} (10^{-9} cm^2 s^{-1}) at 40 °C**	**σ_{Li^+} 10^{-6} (S cm^{-1}) at 40 °C**	**D_{Li+} (10^{-9} cm^2 s^{-1}) at 40 °C**	**σ_{Li^+} 10^{-6} (S cm^{-1}) at 40 °C**
LiTFSI/PEO	1.85	0.80	0.20	0.88
$LiC_{2,2}$TFSI/PEO	2.46	1.00	1.01	4.12
$LiC_{6,6}$TFSI/PEO	3.26	1.14	1.07	3.72

Table S11. Summary of lithium salts properties and their interest in synthesis scalability.

Li Salts	EO:Li	T_{Li^+}	σ_{total} / (S cm^{-1})	LSV / (V)	Synthesis complexity	Scalability	References
LiTFSI	20:1	0.19	8.2×10^{-4} 70 °C	5.4	Easy	Highly	[5]
LiSTFSI	20.5:1	0.93 60 °C	10^{-4} 60 °C	/	Moderate	Moderate	[6]
LiMTFSI	36:1	0.83 70 °C	1.2×10^{-5} 55 °C	4.5	Moderate	Moderate	[7]
LiPBSI	20:1	0.39 60 °C	2.5×10^{-5} 60 °C	/	Easy	Moderate	[8]
LiPHSI	20:1	0.40 60 °C	1.3×10^{-5} 60 °C	/	Easy	Moderate	[8]
LiBTFSI	20:1	0.69 70 °C	3.6×10^{-4} 70 °C	5.8	Moderate	Moderate	[9]
LiTPBTFSI	20:1	0.64 70 °C	1.3×10^{-4} 70 °C	5.0	Moderate	Moderate	[9]
LiDFTFSI	20:1	0.45 70 °C	2.0×10^{-4} 70 °C	5.3	Moderate	Poor	[10]
$LiC_{n,n}TFSI$	20:1	0.39-0.52 70 °C	1.2×10^{-4} 70 °C	4.4	Easy	Promising	This work

REFERENCES

(1) Pronk, S.; Páll, S.; Schulz, R.; Larsson, P.; Bjelkmar, P.; Apostolov, R.; Shirts, M. R.; Smith, J. C.; Kasson, P. M.; Van Der Spoel, D.; Hess, B.; Lindahl, E. GROMACS 4.5: A High-Throughput and Highly Parallel Open Source Molecular Simulation Toolkit. *Bioinformatics* **2013**, 29 (7), 845–854. https://doi.org/10.1093/bioinformatics/btt055.

(2) Meabe, L.; Peña, S. R.; Martinez-Ibañez, M.; Zhang, Y.; Lobato, E.; Manzano, H.; Armand, M.; Carrasco, J.; Zhang, H. Insight into the Ionic Transport of Solid Polymer Electrolytes in Polyether and Polyester Blends. *Journal of Physical Chemistry C* **2020**, 124 (33), 17981–17991. https://doi.org/10.1021/acs.jpcc.0c04987.

(3) Gouveia, A. S. L.; Bernardes, C. E. S.; Tomé, L. C.; Lozinskaya, E. I.; Vygodskii, Y. S.; Shaplov, A. S.; Lopes, J. N. C.; Marrucho, I. M. Ionic Liquids with Anions Based on Fluorosulfonyl Derivatives: From Asymmetrical Substitutions to a Consistent Force Field Model. *Physical Chemistry Chemical Physics* **2017**, *19* (43), 29617–29624. https://doi.org/10.1039/C7CP06081E.

(4) Canongia Lopes, J. N.; Pádua, A. A. H. CL&P: A Generic and Systematic Force Field for Ionic Liquids Modeling. *Theoretical Chemistry Accounts* **2012**, *131* (3), 1129. https://doi.org/10.1007/s00214-012-1129-7.

(5) Martinez-Ibañez, M.; Sanchez-Diez, E.; Oteo, U.; Gracia, I.; Aldalur, I.; Eitouni, H. B.; Joost, M.; Armand, M.; Zhang, H. Anions with a Dipole: Toward High Transport Numbers in Solid Polymer Electrolytes. *Chemistry of Materials* **2022**, *34* (7), 3451–3460. https://doi.org/10.1021/acs.chemmater.2c00285.

(6) Feng, S.; Shi, D.; Liu, F.; Zheng, L.; Nie, J.; Feng, W.; Huang, X.; Armand, M.; Zhou, Z. Single Lithium-Ion Conducting Polymer Electrolytes Based on Poly[(4-Styrenesulfonyl)(Trifluoromethanesulfonyl)Imide] Anions. *Electrochimica Acta* **2013**, *93*, 254–263. https://doi.org/10.1016/j.electacta.2013.01.119.

(7) Porcarelli, L.; Shaplov, A. S.; Salsamendi, M.; Nair, J. R.; Vygodskii, Y. S.; Mecerreyes, D.; Gerbaldi, C. Single-Ion Block Copoly(Ionic Liquid)s as Electrolytes for All-Solid State Lithium Batteries. *ACS Applied Material & Interfaces* **2016**, *8* (16), 10350–10359. https://doi.org/10.1021/acsami.6b01973.

(8) Ryu, S.-W.; Trapa, P. E.; Olugebefola, S. C.; Gonzalez-Leon, J. A.; Sadoway, D. R.; Mayes, A. M. Effect of Counter Ion Placement on Conductivity in Single-Ion Conducting Block Copolymer Electrolytes. *Journal of The Electrochemical Society* **2005**, *152* (1), A158. https://doi.org/10.1149/1.1828244.

(9) Qiao, L.; Rodriguez Peña, S.; Martínez-Ibañez, M.; Santiago, A.; Aldalur, I.; Lobato, E.; Sanchez-Diez, E.; Zhang, Y.; Manzano, H.; Zhu, H.; Forsyth, M.; Armand, M.; Carrasco, J.; Zhang, H. Anion π-π Stacking for Improved Lithium Transport in Polymer Electrolytes. *Journal of the American Chemical Society* **2022**, *144* (22), 9806–9816. https://doi.org/10.1021/jacs.2c02260.

(10) Zhang, H.; Oteo, U.; Judez, X.; Eshetu, G. G.; Martinez-Ibañez, M.; Carrasco, J.; Li, C.; Armand, M. Designer Anion Enabling Solid-State Lithium-Sulfur Batteries. *Joule* **2019**, *3* (7), 1689–1702. https://doi.org/10.1016/j.joule.2019.05.003.